3-1-2022

TRAF2, an innate immune sensor, reciprocally regulates mitophagy and inflammation to maintain cardiac myocyte homeostasis

Xiucui Ma

David R Rawnsley

Attila Kovacs

Moydul Islam

John T Murphy

See next page for additional authors

Authors

Xiucui Ma, David R Rawnsley, Attila Kovacs, Moydul Islam, John T Murphy, Chen Zhao, Minu Kumari, Layla Foroughi, Haiyan Liu, Kevin Qi, Aaradhya Diwan, Krzysztof Hyrc, Sarah Evans, Takashi Satoh, Brent A French, Kenneth B Margulies, Ali Javaheri, Babak Razani, Douglas L Mann, Kartik Mani, and Abhinav Diwan
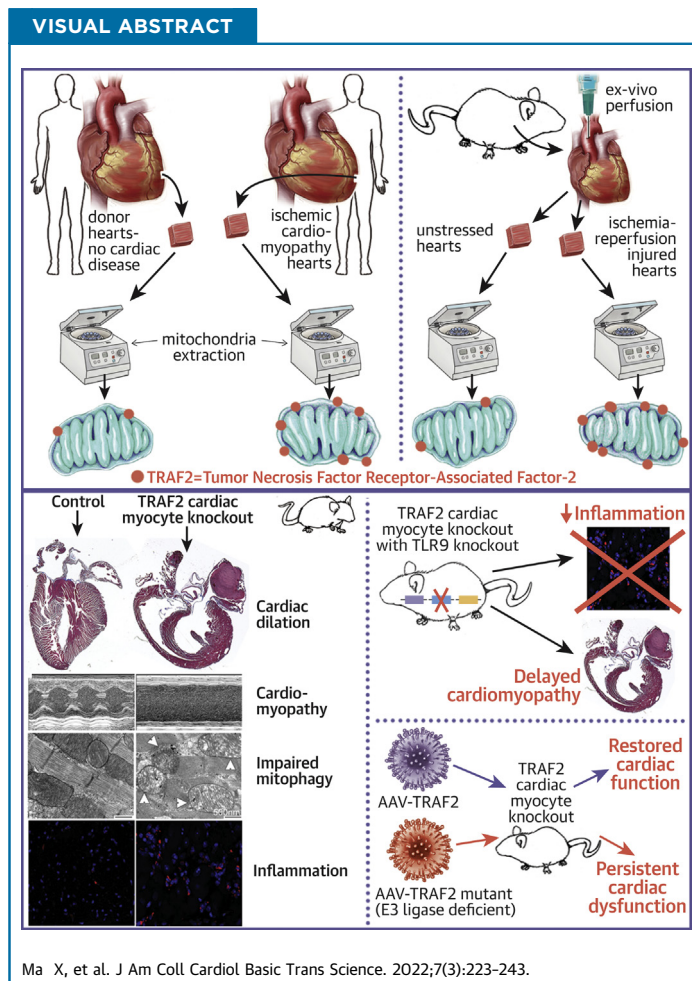
PRECLINICAL RESEARCH

TRAF2, an Innate Immune Sensor, Reciprocally Regulates Mitophagy and Inflammation to Maintain Cardiac Myocyte Homeostasis

Xiucui Ma, PhD,[a,b,*] David R. Rawnsley, MD, PhD,[a,*] Attila Kovacs, MD,[a] Moydul Islam, MS,[a] John T. Murphy, PhD,[a,b]
Chen Zhao, BS,[a] Minu Kumari, PhD,[a] Layla Foroughi, BA,[a,b] Haiyan Liu, MD,[a,b] Kevin Qi,[a] Aaradhya Diwan,[a]
Krzysztof Hyrc, PhD,[c,d] Sarah Evans, PhD,[a] Takashi Satoh, MD, PhD,[e] Brent A. French, PhD,[f]
Kenneth B. Margulies, MD,[g] Ali Javaheri, MD, PhD,[a] Babak Razani, MD, PhD,[a,b] Douglas L. Mann, MD,[a,b,h]
Kartik Mani, MBBS,[a,b,†] Abhinav Diwan, MD[a,b,d,h,i,†]

VISUAL ABSTRACT

Ma X, et al. J Am Coll Cardiol Basic Trans Science. 2022;7(3):223-243.

HIGHLIGHTS

- **TRAF2, an innate immunity adaptor protein, localizes to the mitochondria in cardiac myocytes in human and mouse hearts during physiology, with increased mitochondrial localization under pathologic stress.**

- **TRAF2 is essential for physiological mitophagy in cardiac myocytes, with a critical requirement for its E3 ligase domain in this role.**

- **TRAF2 suppresses expression of TLR9, a sensor for leaked mitochondrial DNA, to suppress sterile inflammation in the myocardium.**

- **Loss of physiological TRAF2-mediated mitophagy in cardiac myocytes triggers myocardial inflammation and cardiac myocyte cell death. Interruption of TLR9-mediated mitochondrial DNA sensing rescues inflammation, but persistence of damaged mitochondria leads to cell death with aging, pointing to a critical role for physiological cardiac myocyte mitophagy in maintaining myocardial homeostasis.**

ABBREVIATIONS AND ACRONYMS

AAV9 = adeno-associated virus serotype 9

cTnT = cardiac troponin T

ER = endoplasmic reticulum

FS = fractional shortening

GFP = green fluorescent protein

IP = intraperitoneal

LV = left ventricular

MAM = mitochondria-associated membranes

MCM = MerCreMer

MEF = murine embryonic fibroblast

PINK1 = PTEN-induced kinase 1

RFP = red fluorescent protein

TLR9 = toll-like receptor 9

TRAF2 = tumor necrosis factor receptor-associated factor-2

TUNEL = terminal deoxynucleotidyl transferase dUTP nick end labeling

SUMMARY

Mitochondria are essential for cardiac myocyte function, but damaged mitochondria trigger cardiac myocyte death. Although mitophagy, a lysosomal degradative pathway to remove damaged mitochondria, is robustly active in cardiac myocytes in the unstressed heart, its mechanisms and physiological role remain poorly defined. We discovered a critical role for TRAF2, an innate immunity effector protein with E3 ubiquitin ligase activity, in facilitating physiological cardiac myocyte mitophagy in the adult heart, to prevent inflammation and cell death, and maintain myocardial homeostasis. (J Am Coll Cardiol Basic Trans Science 2022;7:223–243) Published by Elsevier on behalf of the American College of Cardiology Foundation. This is an open access article under the CC BY-NC-ND license (http://creativecommons.org/licenses/by-nc-nd/4.0/).

Mitochondrial permeabilization results in activation of cell death signaling and is a major pathway for cardiac myocyte death under stress.[1] Damaged mitochondria also leak mitochondrial DNA, which is a potent trigger for immune activation due to its physical features that mimic bacterial DNA.[1] Indeed, mitochondrial damage resulting in sterile myocardial inflammation and cardiac myocyte death is implicated in causing cardiomyopathy under pressure overload stress[2,3] and with ischemia-reperfusion injury,[4,5] whereby targeting cell death as well as deleterious myocardial inflammation are regarded as key therapeutic targets to prevent and treat heart failure.[1,6] Mitophagy is a lysosomal process to sequester damaged mitochondria (or parts thereof) to facilitate their removal via lysosomal degradation, and serves as a defense mechanism against mitochondrial DNA sensing to drive inflammation and cell death.[2,7]

Mitophagy plays a critical role in the myocardium during perinatal cardiac growth and development,[8] with aging,[9,10] with exhaustive exercise,[7] and in pathologic states, such as after injury.[2,9-15] Despite these discoveries, its role in physiological function of the adult heart remains unknown. Moreover, although studies with contemporary reporters demonstrate robust rates of cardiac myocyte mitophagy in the unstressed myocardium,[16,17] ablation of canonical mitophagy mediators such as PTEN-induced kinase 1 (PINK1) and PARKIN[18] does not alter mitophagy in young adult mouse hearts.[12,15,19-21]

Prior studies indicate that lysosome function is critical for preventing myocardial inflammation under stress, as ablation of lysosomal DNase II in cardiac myocytes, which degrades mitochondrial DNA, exacerbates myocardial inflammation to accelerate development of cardiomyopathy with pressure overload.[2] Whether physiological mitophagy suppresses myocardial inflammatory signaling in the unstressed heart remains unknown. It is also noteworthy that all currently defined mitophagy pathways are intrinsic to damaged mitochondria and recognize mitochondrial damage or dysfunction to facilitate lysosomal removal of damaged mitochondria via mitophagy or other mechanisms,[22] whereby participation of innate immune mechanisms in facilitating mitophagy remains a missing piece of this conceptual framework. In this paper, we reveal evidence that tumor necrosis factor receptor-associated factor-2 (TRAF2), an innate immunity effector, acts as a first line of defense

From the ªCenter for Cardiovascular Research and Cardiovascular Division, Department of Internal Medicine, Washington University School of Medicine, St. Louis, Missouri, USA; ᵇJohn Cochran VA Medical Center, St. Louis, Missouri, USA; ᶜAlafi Neuroimaging Laboratory, Washington University School of Medicine, St. Louis, Missouri, USA; ᵈHope Center for Neurological Disorders, Washington University School of Medicine, St. Louis, Missouri, USA; ᵉDepartment of Immune Regulation, Tokyo Medical and Dental University (TMDU), Tokyo, Japan; ᶠDepartment of Biomedical Engineering, University of Virginia, Charlottesville, Virginia, USA; ᵍDepartment of Medicine, University of Pennsylvania, Philadelphia, Pennsylvania, USA; ʰDepartment of Cell Biology and Physiology, Washington University School of Medicine, St. Louis, Missouri, USA; and the ⁱDepartment of Obstetrics and Gynecology, Washington University School of Medicine, St. Louis, Missouri, USA. *Drs Ma and Rawnsley contributed equally to this work as first authors. †Drs Mani and Diwan are joint senior authors.

Junichi Sadoshima, MD, served as Guest Associate Editor for this paper. Michael Bristow, MD, served as Guest Editor-in-Chief for this paper.


FIGURE 1 **TRAF2 Localizes to the Mitochondria in Human and Mouse Hearts**
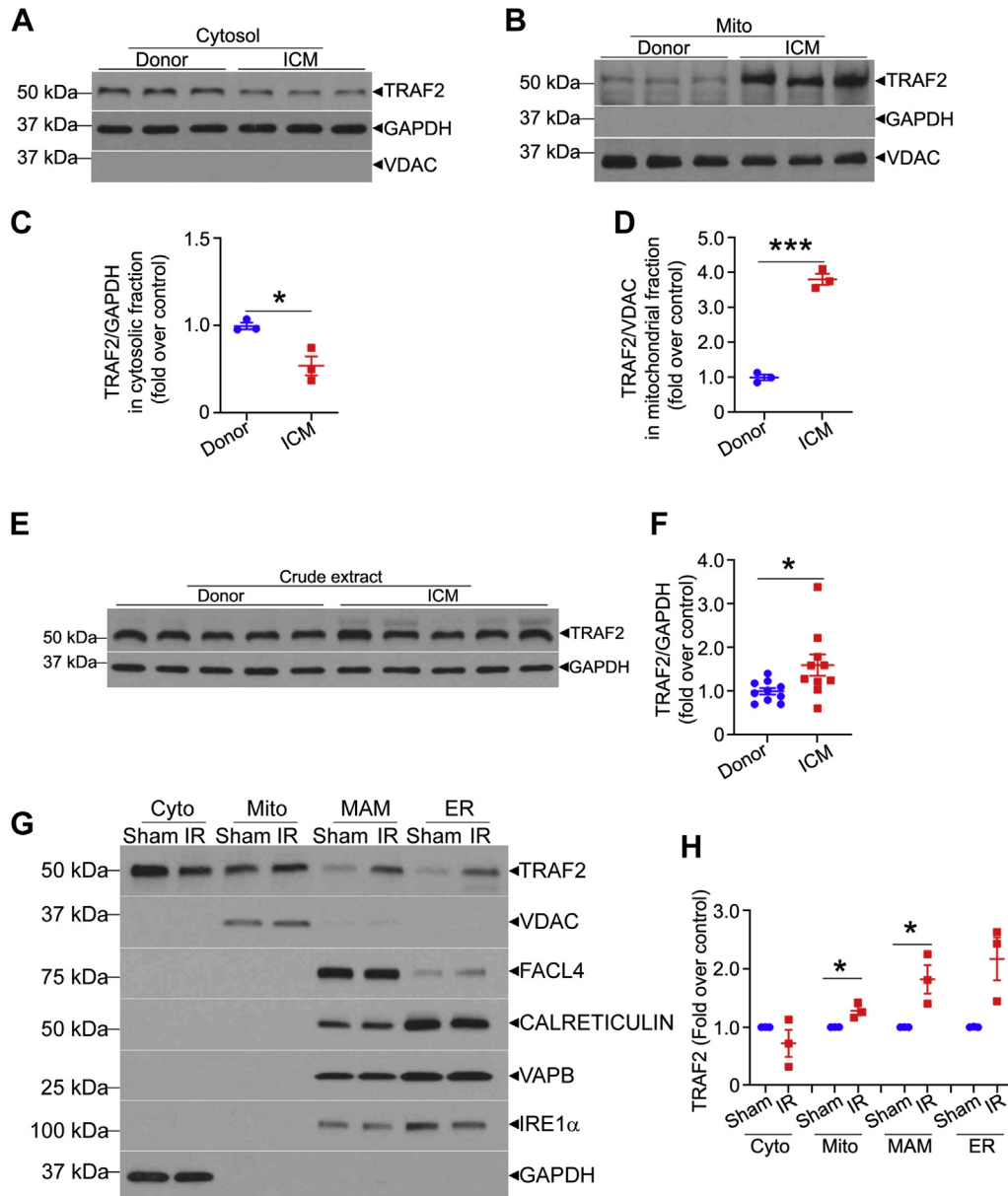
(A and B) Immunoblots depicting TRAF2 expression in hearts from individuals evaluated as donors for cardiac transplantation, without ev-idence for cardiomyopathy (donor) or patients with end-stage ischemic cardiomyopathy (ICM) undergoing cardiac transplantation. The hearts were subjected to biochemical fractionation into mitochondria-enriched **(B)** and cytosolic **(A)** fractions, shown by segregation of VDAC, a mitochondrial protein and GAPDH, a cytosolic protein, respectively. **(C and D)** Quantitative assessment of TRAF2 expression in the respective biochemical fractions are shown in **A and B**. **(E and F)** Representative immunoblot and quantitation are shown depicting total TRAF2 expression in crude extracts from human hearts from patients with ischemic cardiomyopathy (ICM) or donors as control. **(G and H)** Representative immunoblot is shown depicting TRAF2 expression in hearts from male C57BL/6J mice (8 weeks old) subjected to ex vivo ischemia-reperfusion injury (IR) or sham (S) treatment as control. Expression of VDAC, FACL4, calreticulin, VAPB, and IRE1α is shown to evaluate cosegregation with mitochondria (mito, with VDAC), mitochondria-associated membranes (MAM, with FACL4), endoplasmic re-ticulum (ER, with calreticulin, VAPB, and IRE1α), and cytosol (cyto, with GAPDH). *$P < 0.05$ and ***$P < 0.001$, by *t*-test. No statistically significant differences were observed between the groups for TRAF2 abundance in the cyto fraction (by *t*-test) or ER (by Mann-Whitney test).

FIGURE 2   **TRAF2 Ablation in Adult Cardiac Myocytes Induces Cardiomyopathy With Damaged Mitochondria and Cell Death**
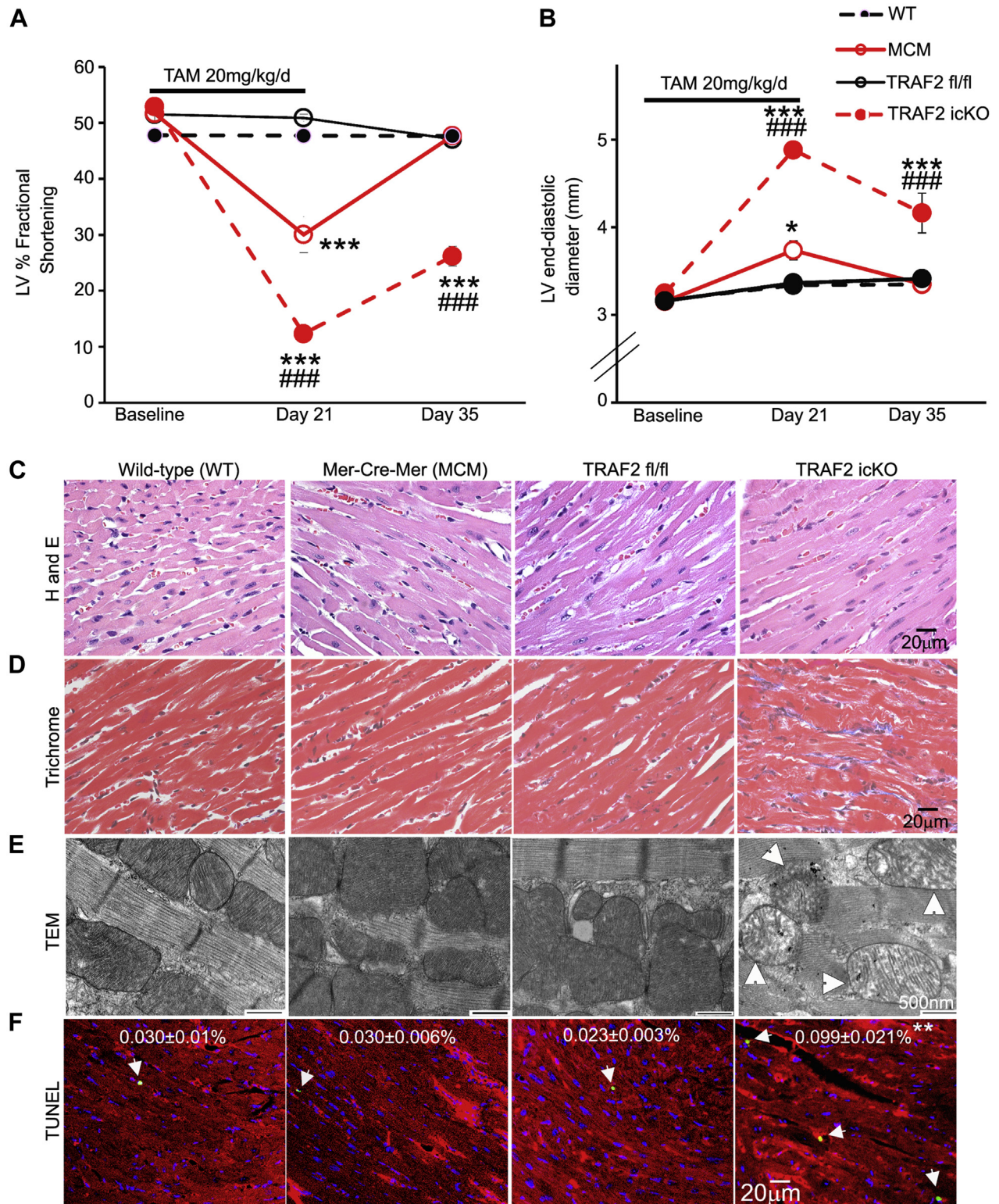
against cardiac myocyte cell death and sterile myocardial inflammation by facilitating mitophagy in the adult mouse heart.

Our data demonstrate that a fraction of TRAF2 is associated with mitochondria in homeostasis, and its recruitment to the mitochondria is up-regulated under conditions of mitochondrial damage with ischemia-reperfusion injury and in cardiomyopathic failing human hearts. Inducible ablation of TRAF2 in adult cardiac myocytes impairs mitophagy and provokes accumulation of damaged mitochondria, primarily based upon its role as an E3 ubiquitin ligase. Moreover, inducible TRAF2 ablation up-regulates toll-like receptor 9 (TLR9) expression to drive myocardial dysfunction and knockout of TLR9 delays the onset of cardiomyopathy by curtailing inflammation, but does not prevent eventual cardiomyopathic decompensation due to presence of damaged mitochondria. These studies highlight a central role for the innate immunity pathway as a mitochondria-extrinsic mechanism in sensing mitochondrial damage to effect mitophagy and maintain homeostasis.

METHODS

REAGENTS AND SAMPLES.
We crossed mice homozygous for floxed *Traf2* alleles (*Traf2* fl/fl)[23] (which permits Cre-mediated excision of exon 3 and introduces a frame shift resulting in loss of TRAF2 protein; generously provided by Dr. Robert Brink, Garvan Institute of Medical Research, Australia) with mice carrying the *Myh6* promoter driven Mer-Cre-Mer (MCM) transgene (generous gift from Jeffery D. Molkentin, PhD, Cincinnati Children's Hospital, Cincinnati, Ohio).[24] Mice were injected with tamoxifen (Millipore Sigma #T5648, dissolved in ethanol and sunflower oil #S5007 to make a stock solution of 10 mg/mL) at the doses indicated (intraperitoneal [IP]); or fed with tamoxifen chow (Envigo, cat#TD.130857), as described for individual experiments. *Tlr9*-null mice were generously provided by

Drs. Shizou Akira, Laboratory of Host Defense, Research Institute for Microbial Diseases, Osaka University, Osaka, Japan. MitoQC reporter strain was previously described[17] and generously provided by Dr. Ian Ganley at University of Dundee, UK. *Park2*-null (Strain number 006582), *Pink1*-null (stock number 017946), and the autophagic reporter CAG-RFP-EGFP-LC3 (strain number 027139) mice were purchased from The Jackson Laboratory. All mice were maintained on a C57BL/6J background. Mice of both sexes were studied. No significant differences were observed between sexes for the primary phenotype, thus data for both sexes were combined for presentation. Mouse studies were randomized and observers blinded. All animal studies were approved by the institutional animal care and use committee at Washington University School of Medicine. Studies on human tissue were performed under an exemption by the institutional review board at Washington University School of Medicine because only deidentified human samples were used. Human heart tissue was obtained from Kenneth Margulies, MD, at the University of Pennsylvania, Philadelphia (Supplemental Table 1). Hearts were categorized as either nonfailing (no history of heart failure, obtained from nonfailing brain-dead donors) or ischemic cardiomyopathy (obtained at time of orthotopic heart transplantation). After in situ cold cardioplegia, all hearts were placed on wet ice at 4°C in Krebs-Henseleit buffer. Transmural left ventricular (LV) samples were obtained from the LV free wall with epicardial fat excluded. The mitoKeima construct was generously provided by Dr. Atsushi Miyawaki, RIKEN brain science institute in Saitama, Japan.

ECHOCARDIOGRAPHY AND MYOCARDIAL CHARACTERIZATION.
Two-dimensional-directed M-mode echocardiography was performed as we have previously described.[25] Histologic assessment for myocyte registration was performed with hematoxylin and eosin staining, and myocardial fibrosis was assessed

---

FIGURE 2   Continued

(A and B) Left ventricular (LV) endocardial fractional shortening (%FS **(A)** and end-diastolic diameter **(B)** in wild-type, *Traf2* floxed (TRAF2 fl/fl), MerCreMer (MCM) mice, and mice homozygous for *Traf2* floxed alleles carrying the MerCreMer transgene (to generate TRAF2-icKO), 14 days after tamoxifen treatment (20 mg/kg/d, IP 5 days per week for 3 weeks). n = 9 to 10 mice per group. *P < 0.05 and ***P < 0.001 for comparison versus wild-type group; ###P < 0.001 for comparison versus *Traf2* fl/fl group by post hoc test after 2-way ANOVA. **(C and D)** Representative images with hematoxylin and eosin (H and E) staining **(C)**, and trichrome staining **(D)** to evaluate myocardial structure and fibrosis, respectively, in mice as treated in **A** and **B**. **(E)** Representative transmission electron microscopy images to evaluate myocardial ultrastructure in mice as in **A**. **Arrows** indicate swollen mitochondria with cristal rarefication. **(F)** Representative TUNEL-stained images to evaluate cardiac myocyte TUNEL positivity **(green)** in mice as in **A**. DAPI staining identifies nuclei. Staining for α-sarcomeric actin was performed to evaluate TUNEL staining in cardiac myocyte nuclei. %TUNEL-positive nuclei/total cardiac myocyte nuclei are depicted. n = 4 to 6/group. **P < 0.01 versus *Traf2* fl/fl by post hoc test after 1-way ANOVA. ANOVA = analysis of variance; TAM = tamoxifen; TEM = transmission electron microscopy; TUNEL = terminal deoxynucleotidyl transferase dUTP nick end labeling; WT = wild type.

FIGURE 3   TRAF2 Ablation in Adult Cardiac Myocytes Impairs Homeostatic Mitophagy
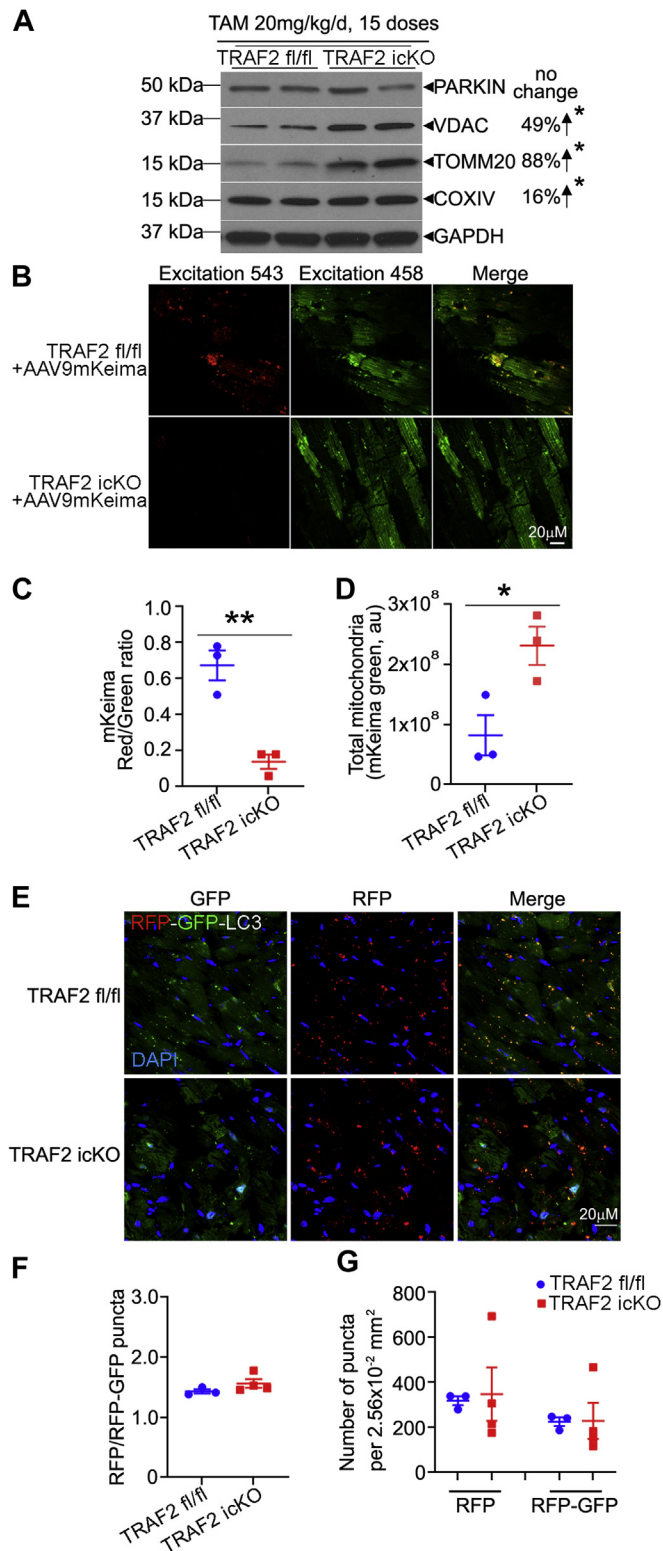
with Masson's trichrome staining, as we have previously described.[25] Quantitative assessment of fibrosis was performed with Picrosirius Red staining, and images were assessed for area of the red signal as a fraction of total tissue area by Visiomorph software (Visiopharm). Transmission electron microscopy was performed in cardiac tissue as previously described.[25]

STUDIES WITH ADENO-ASSOCIATED VIRAL VECTORS.
Adeno-associated virus serotype 9 [AAV9] particles coding for TRAF2 or its Rm mutant constructs (which we have described previously[26]) driven by the cardiac troponin T (cTnT) promoter for conferring cardiac myocyte selective expression,[27] were generated by the Hope Center viral vectors core; using AAV backbone constructs generously provided by Dr. Brent French at University of Virginia, Charlottesville.

EX VIVO CARDIAC ISCHEMIA-REPERFUSION INJURY.
Hearts were isolated and perfused as previously described.[28] After a 20-minute stabilization period, mouse hearts were subjected to no-flow ischemia (time [t] = 0 minutes) for 30 minutes followed by reperfusion for 60 minutes (total t = 90 minutes).

ADULT CARDIAC MYOCYTE ISOLATION.
Adult mouse hearts were subjected to enzymatic digestion to isolate adult cardiac myocytes, as described.[29] The remaining cellular fraction was isolated as the non-myocyte fraction. The cells were subsequently homogenized in RIPA buffer and subjected to SDS-PAGE gel electrophoresis followed by immunoblotting as we have previously described.[26]

PREPARATION OF MURINE EMBRYONIC FIBROBLASTS.
Traf2 floxed or *Pink1* floxed mice were subjected to timed mating and murine embryonic fibroblasts were prepared from embryonic day 14 pups following standard protocols.

BIOCHEMICAL SUBCELLULAR FRACTIONATION.
Mitochondria-enriched and cytosolic fractions were prepared from hearts and cells following the protocols we have previously described.[26] Biochemical separation of mitochondria-rich fraction into mitochondria stripped of other organelles, mitochondria-associated membranes (MAM), and endoplasmic reticulum (ER) was performed with Percoll density centrifugation following published protocols.[30]

IN SITU HYBRIDIZATION WITH RNAscope.
All procedures for *Tlr9* transcript detection with fluorescence in situ hybridization were performed using the RNAscope Multiplex Fluorescent Reagent kit V2 (Cat. No. 323100, Advanced Cell Diagnostics) according to the manufacturer's instructions. RNAscope Probe-Mm-Tlr9, Mouse (Cat. No. 468281, Advanced Cell Diagnostics) and Opal 690 Dye (Cat. No. FP1497001KT, Akoya BioSciences) were used according to the manufacturer's instructions for fluorescence in situ hybridization. Desmin staining was performed subsequently to the horseradish peroxidase blocker step of fluorescence in situ hybridization. Slides were rinsed and covered with 1:50 dilution of goat polyclonal anti-desmin antibody (Cat. No. SC-7559, Santa Cruz Biotechnology) overnight at 4°C. The next morning, slides were rinsed and covered with 1:200 dilution of Alexa Fluor 488 donkey anti-goat secondary antibody (Cat. No. A-11055, Invitrogen) for 45 min at room temperature. Slides were rinsed and mounted, stained with DAPI using Antifade Mounting Medium with DAPI (Cat. No. H-1200, Vector Labs). Slides were stored at 4°C in the dark until image analysis. Images were captured on a Zeiss LSM 700 confocal microscope.

IMMUNOFLUORESCENCE ANALYSIS.
We followed the protocol we have previously described.[25] Paraffin-embedded heart sections (10-μm thick) were subjected to heat-induced epitope retrieval, followed by blocking, and then incubated overnight with primary antibody. After serial washes, samples were stained with Alexa Fluor 594 (Invitrogen) and mounted with fluorescent DAPI mounting medium (Vector Labs,

---

FIGURE 3 Continued

(A) Representative immunoblot is shown depicting expression of PARKIN and mitochondrial proteins (VDAC, TOMM20, COXIV) in cardiac extracts from mice at day 35 after inducible adult-onset ablation of TRAF2 (TRAF2-icKO), 14 days after tamoxifen (TAM) treatment (20 mg/kg/d, intraperitoneal for 5 days per week for 3 weeks). n = 4/group. Protein levels were normalized to GAPDH. **Upward arrow** points to upregulation in abundance of indicated protein indicated as a % change. *P < 0.05 for TRAF2-icKO versus *Traf2* fl/fl groups by *t*-test; and. **(B to D)** Representative images **(B)** from hearts transduced with AAV9-mitoKeima in mice as in **A**; with the ratio of quantitation of mitoKeima emission in the red channel over green as an index of mitophagy **(C)**. Total mitochondria were assessed by abundance of the green signal (arbitrary units, au) per unit area of transduced myocytes **(D)**. *P < 0.05 and **P < 0.01 by *t*-test. **(E-G)** Representative images **(E)** for assessment of flux through macroautophagy in TRAF2-icKO versus *Traf2* fl/fl mice carrying the RFP-GFP-LC3 reporter transgene, with quantitative assessment of the ratio of autolysosomes (punctate RFP signal) to autophagosomes (punctate RFP+GFP signal, in **F**); and total autophagosomes (RFP+GFP puncta) and autolysosomes (RFP puncta) per unit myocardial area in **G**. No statistically significant differences were observed between TRAF2-icKO versus *Traf2* fl/fl mice by *t*-test in **F and G**. GFP = green fluorescent protein; RFP = red fluorescent protein.

FIGURE 4   TRAF2 Ablation in Adult Cardiac Myocytes Up-Regulates TLR9 and Mitochondrial DNA Sensing
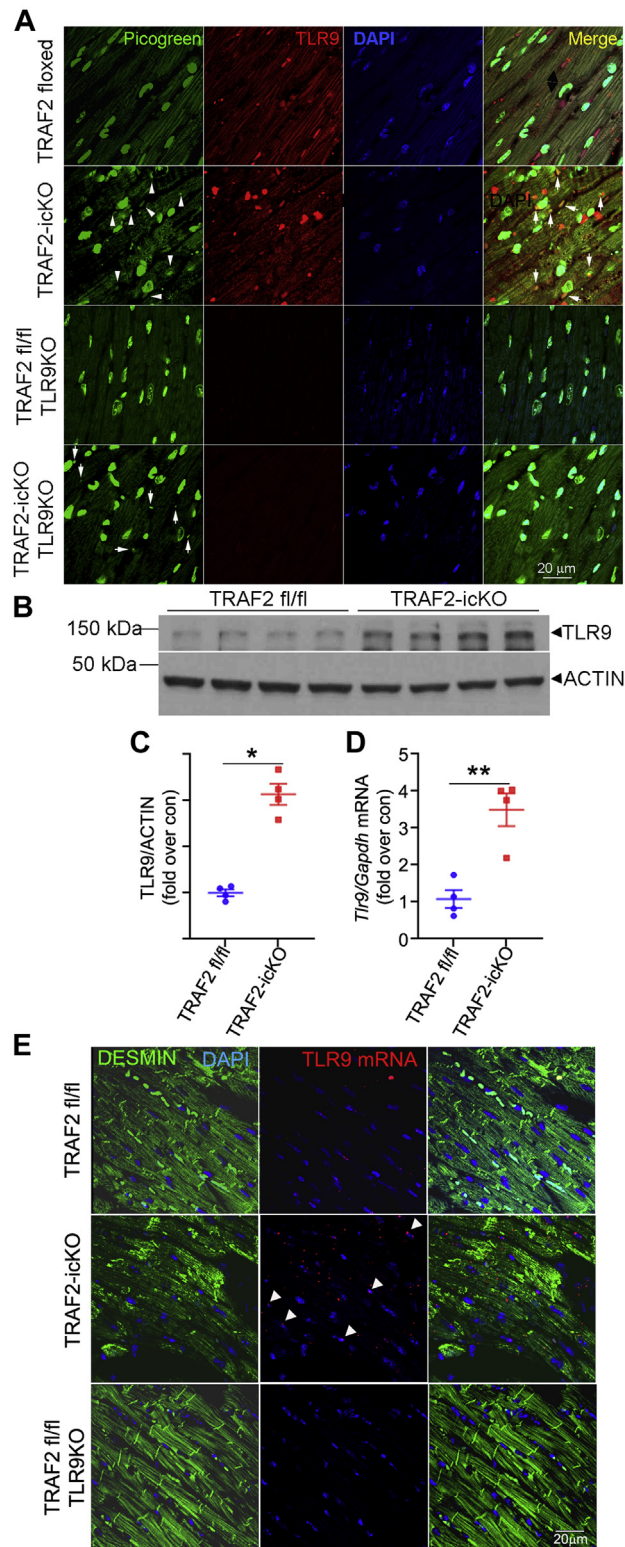
H-1200). Confocal imaging was performed on a Zeiss confocal LSM-700 laser scanning confocal microscope using 639 Zeiss Plan-Neofluar 40/1.3 and 63/1.4 oil immersion objectives, and images were acquired using Zen 2010 software. CD68 (Biolegend, 137001), TLR9 (Novus Biologicals, NBP2-24729), PicoGreen from Quant-iT PicoGreen dsDNA Assay Kit (Thermo Fisher Scientific, P7589). For CD68 staining, we used MaxBlock Autofluorescence Reducing Reagent Kit (MaxVision Biosciences, cat# MB-M) to block the high autofluorescence background.

TUNEL STAINING. Terminal deoxynucleotidyl transferase dUTP nick end labeling (TUNEL) was performed on formalin-fixed and paraffin-embedded tissue sections by using the Dead-End fluorometric TUNEL system (Promega, G3250) following the manufacturer's directions, as previously described.[25]

ASSESSMENT OF AUTOPHAGIC FLUX. We performed autophagic flux analyses by immunofluorescence examination of frozen myocardial tissue from mice with expression of the red fluorescent protein (RFP)-green fluorescent protein (GFP)-LC3 reporters, as described.[31] Only puncta associated with cells identified as myocytes based upon visualization of boxcar-shaped nuclei were counted.

ASSESSMENT OF MITOPHAGY. Mice transduced with AAV9 particles coding for CMV promoter-driven mitoKeima were generated by the Hope Center viral vectors core at Washington University at a dose of 3.5×10^{11} viral particles per mouse. Mitophagy was assessed with expression of mitoKeima as previously described.[16,32] Briefly, live imaging of freshly harvested cardiac slices were performed with a Zeiss LSM5 Pascal confocal microscope. Two sequential excitations were performed at wavelengths of 458 and 543 nm, followed by imaging with a 560-nm longpass filter for assessment of the mitophagy signal. Laser power was individualized for each condition to optimize Keima imaging. Murine embryonic fibroblasts (MEFs) were transfected with pcDNA3.1 encoding for mitoKeima construct using GenJet transfection reagent (Sinagen) following the manufacturer's protocols, and mitophagy was assessed with sequential excitation at wavelengths at 458 and 561 nm, followed by emission at 580 nm using a Nikon A1R confocal system at the Washington University Center for Cellular Imaging. Adenoviruses expressing Cre and rat PARKIN were generated as previously described.[26] The images were quantitated using ImageJ software (NIH). Mitophagy was also assessed after injection of AAV9-cTnT-TRAF2 or AAV9-cTnT-null viral particles (with 3.5×10^{11} viral particles per mouse) in young adult mitoQC mice. Mitophagy index was calculated as a ratio of the average intensity of the red/green signal using ImageJ software.

QUANTITATIVE POLYMERASE CHAIN REACTION ANALYSES. Assessment of transcript abundance was performed as previously described[25] using SYBR Green with primers reported in Supplemental Table 2. Assessment of *Pink1* transcript expression was performed using TaqMan gene expression assays (Applied Biosystems) for mouse Pink1 (Mm00550827_m1).

IMMUNOBLOTTING. Immunoblotting was performed as previously described.[25] Specific antibodies employed are as follows: LC3 (Novus Biologicals, NB100-2220); p62 (Abcam, ab56416); TRAF2 (Abcam, ab126758); COX IV (Abcam, ab14744); TOMM20 (Sigma, WH0009804M1); VDAC (Cell Signaling Technology, 4661S); PARKIN (Abcam, ab15954); FACL4 (Abcam, ab155282); calreticulin Antibody #2891; VAPB (Thermo Fisher Scientific, A302-894A); IRE1α (14C10) (Cell Signaling Technology, 3294S); GAPDH (Abcam, ab22555); TLR9 (Novus Biologicals, NBP2-24729); actin (Sigma, A2066); PINK1 (MRC PPU products and reagents, S774C [DU17570] and S086D [DU34559]); and α-sarcomeric actin (Abcam, ab52219).

ENZYME-LINKED IMMUNOSORBENT ASSAYS. Enzyme-linked immunosorbent assays were performed on sera collected from mice at terminal bleed with the following kits per the manufacturers'


FIGURE 4 Continued

(A) Representative images demonstrating colocalization of PicoGreen with TLR9 in myocardial sections from mice with adult-onset inducible TRAF2 ablation (TRAF2-icKO) and *Traf2* floxed control mice, without and with concomitant germline TLR9 ablation. Nuclei are stained **blue** (DAPI). **Arrowheads** demonstrate colocalization of PicoGreen with TLR9. **Arrows** point to cytosolic detection of DNA by PicoGreen in TRAF2-icKO-TLR9KO myocardium. **(B and C)** Immunoblot **(B)** and quantitation **(C)** depicting TLR9 expression in cardiac extracts from TRAF2-icKO and *Traf2* floxed control mice modeled as in **A**. *$P < 0.05$ and **$P < 0.01$ by t-test. **(D)** *Tlr9* transcript expression in cardiac extracts from TRAF2-icKO and *Traf2* floxed control mice as in **A**. The *P* value depicted is by t-test. **(E)** In situ hybridization to detect *Tlr9* transcript **(red)** and its colocalization with DESMIN **(green)** to identify cardiac myocytes. **Arrowheads** point to TLR9 transcripts in cardiac myocytes. Representative section from *Traf2* fl/fl *Tlr9*-null mouse is shown as a control.

FIGURE 5   TLR9 Ablation Rescues Inflammatory Cell Infiltration and Cell Death in Mice With Inducible TRAF2 Ablation in Adult Cardiac Myocytes, in the Short Term
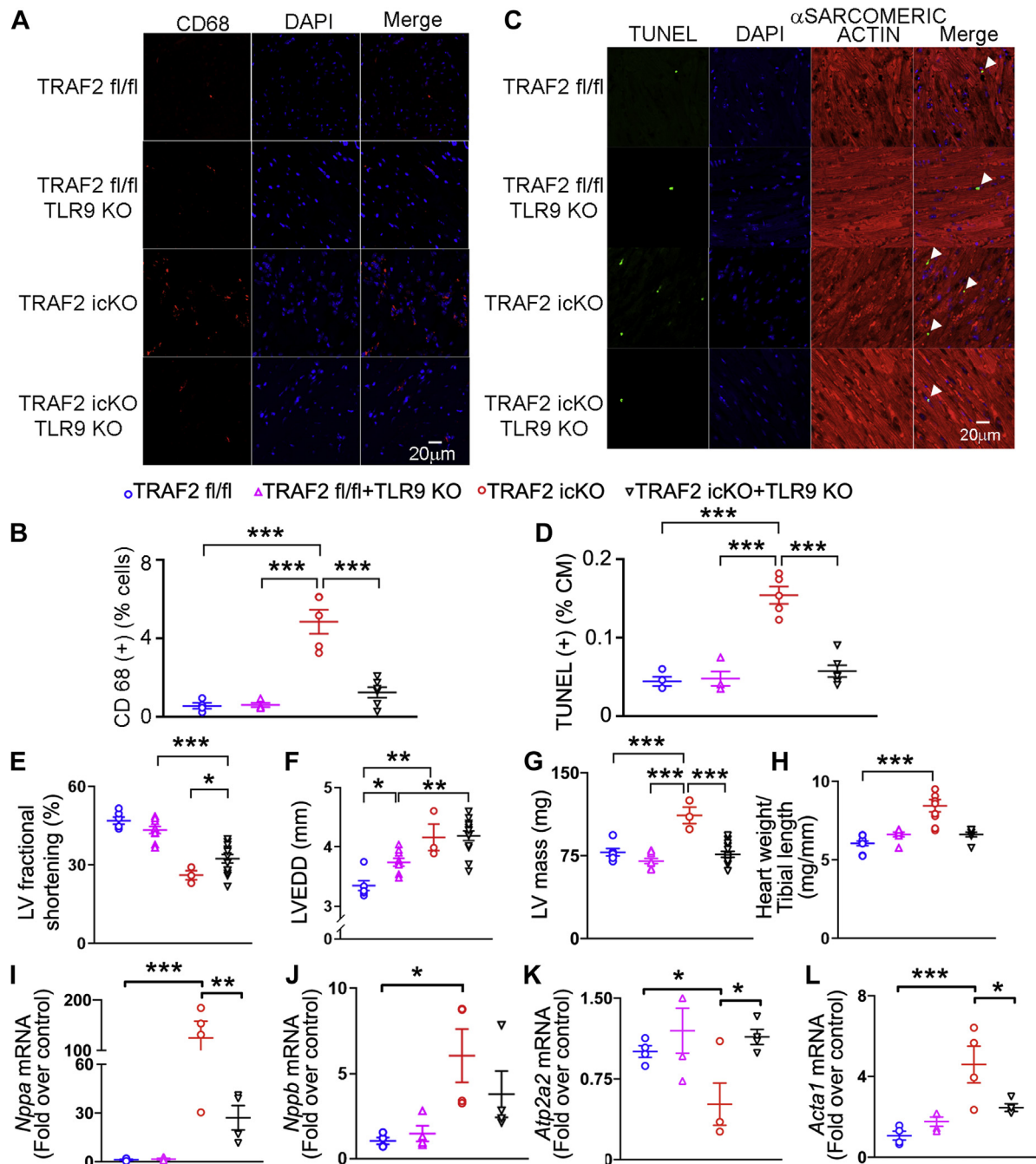
(A) Representative images depicting CD68^{+} cells in myocardial section from mice with adult-onset inducible TRAF2 ablation (TRAF2-icKO) and *Traf2* floxed control mice, without and with concomitant germline TLR9 ablation, 2 weeks after TRAF2 ablation. Nuclei are stained **blue** (DAPI). (B) Quantitation of CD68^{+} cells is shown as % of all DAPI-stained nuclei in mice as in **A**. *P* values are by post hoc test after 1-way ANOVA. **(C and D)** Representative TUNEL-stained images **(C)** with quantitative assessment **(D)** of cardiac myocyte TUNEL positivity (**green**; %TUNEL-positive nuclei/total cardiac myocyte [CM] nuclei) in mice as in **A**. DAPI staining identifies nuclei. Staining for α-sarcomeric actin was performed to evaluate TUNEL staining in cardiac myocyte nuclei. *P* values are by post hoc test after 1-way ANOVA. **(E to H)** Left ventricular endocardial fractional shortening (%FS, **E**), end-diastolic diameter (LVEDD, in millimeters, **F**), LV mass (in milligrams, **G**), and heart weight normalized to tibial length (in milligrams per millimeter, **H**) in mice modeled as in **A**. *P* values are by post hoc test after 1-way ANOVA. **(I-L)** Expression of *Nppa* **(I)**, *Nppb* **(J)**, *Atp2a2* **(K)**, and *Acta1* **(L)** transcripts in mice modeled as in **A**. *$P < 0.05$, **$P < 0.01$, and ***$P < 0.001$ by post hoc test after 1-way ANOVA for all panels except by Kruskal-Wallis test for **H and J**. Abbreviations as in **Figure 2**.

FIGURE 6 TLR9 Ablation Does Not Rescue Mitochondrial Abnormalities and Does Not Prevent Cardiomyopathy With Inducible Cardiac Myocyte TRAF2 Ablation With Longer-Term Follow-Up
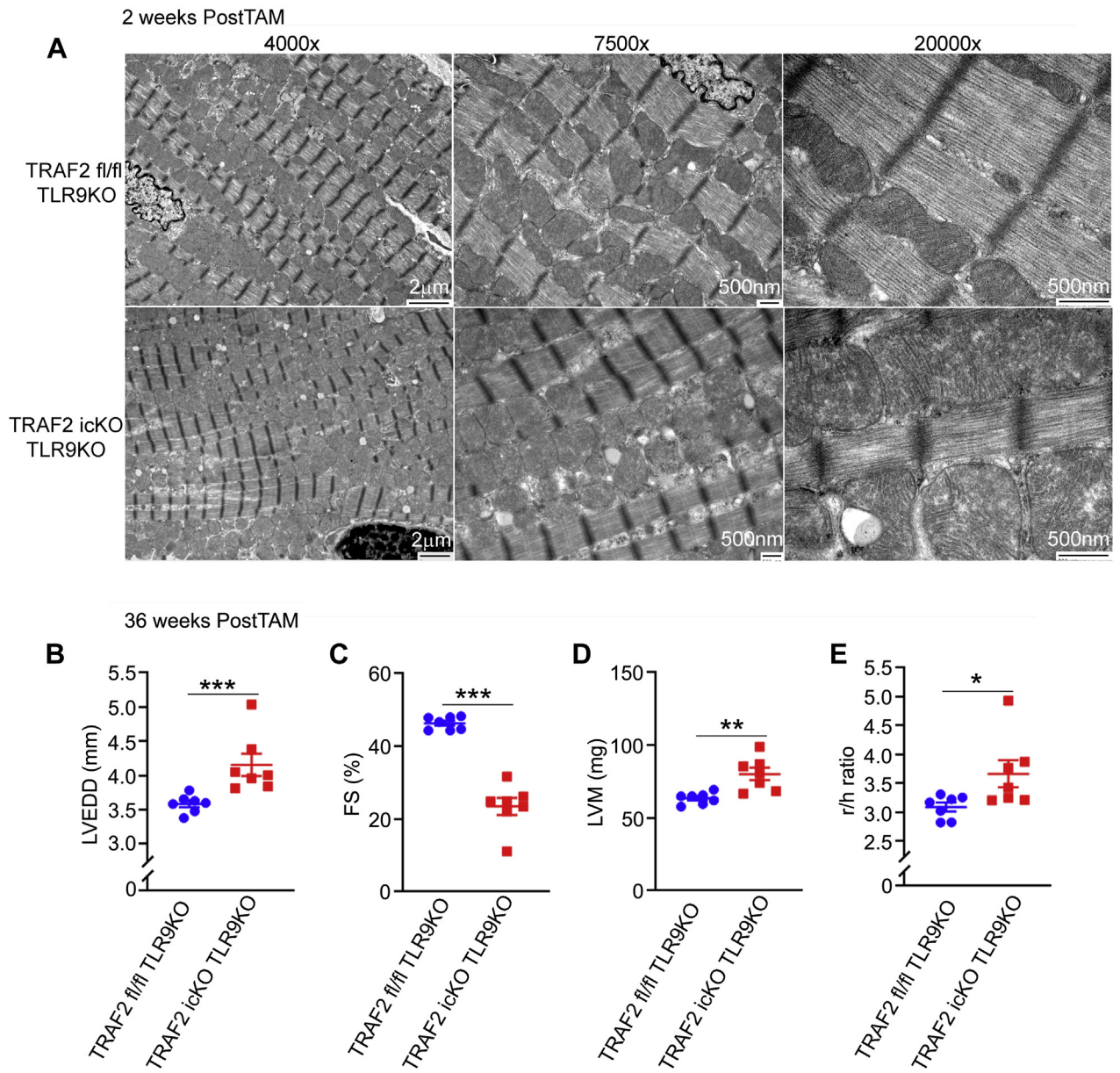

(A) Representative transmission electron microscopy images to evaluate myocardial ultrastructure in mice as with adult-onset inducible TRAF2 ablation (TRAF2-icKO) and *Traf2* floxed control mice, without and with concomitant germline TLR9 ablation, 2 weeks after TRAF2 ablation. (B to E) Mice with adult-onset inducible TRAF2 ablation or *Traf2* floxed alleles in TLR9-null (knockout [KO]) background (TRAF2-icKO TLR9KO and TRAF2 fl/fl TLR9KO) were followed by echocardiographic evaluation at 36 weeks after tamoxifen (TAM) treatment to induce TRAF2 ablation. Left ventricular end-diastolic diameter (LVEDD, mm (B), endocardial fractional shortening (% FS) (C), mass (LVM, in milligrams (D), and ratio of the chamber diameter to wall thickness (r/h) (E) was assessed as shown. *$P < 0.05$, **$P < 0.01$, and ***$P < 0.001$ by *t*-test.

instructions: mouse IL-1β/IL-1F2 (R&D Systems, MLB00C), mouse TNF-alpha (R&D Systems, MTA00B), mouse IL-6 (R&D Systems, M6000B), and HMGB1 (Chondrex, 6010).

IMMUNOGOLD DETECTION. For immunolocalization, cells were fixed in 4% paraformaldehyde/0.05% glutaraldehyde (Polysciences) in 100 mmol/L PIPES/ 0.5 mmol/L MgCl$_2$, pH 7.2 for 1 hour at 4°C. Samples

FIGURE 7   Restoration of TRAF2, but Not Its E3 Ligase–Deficient Mutant, Rescues Cardiomyopathy and Mitochondrial Abnormalities With Inducible Cardiac Myocyte TRAF2 Ablation
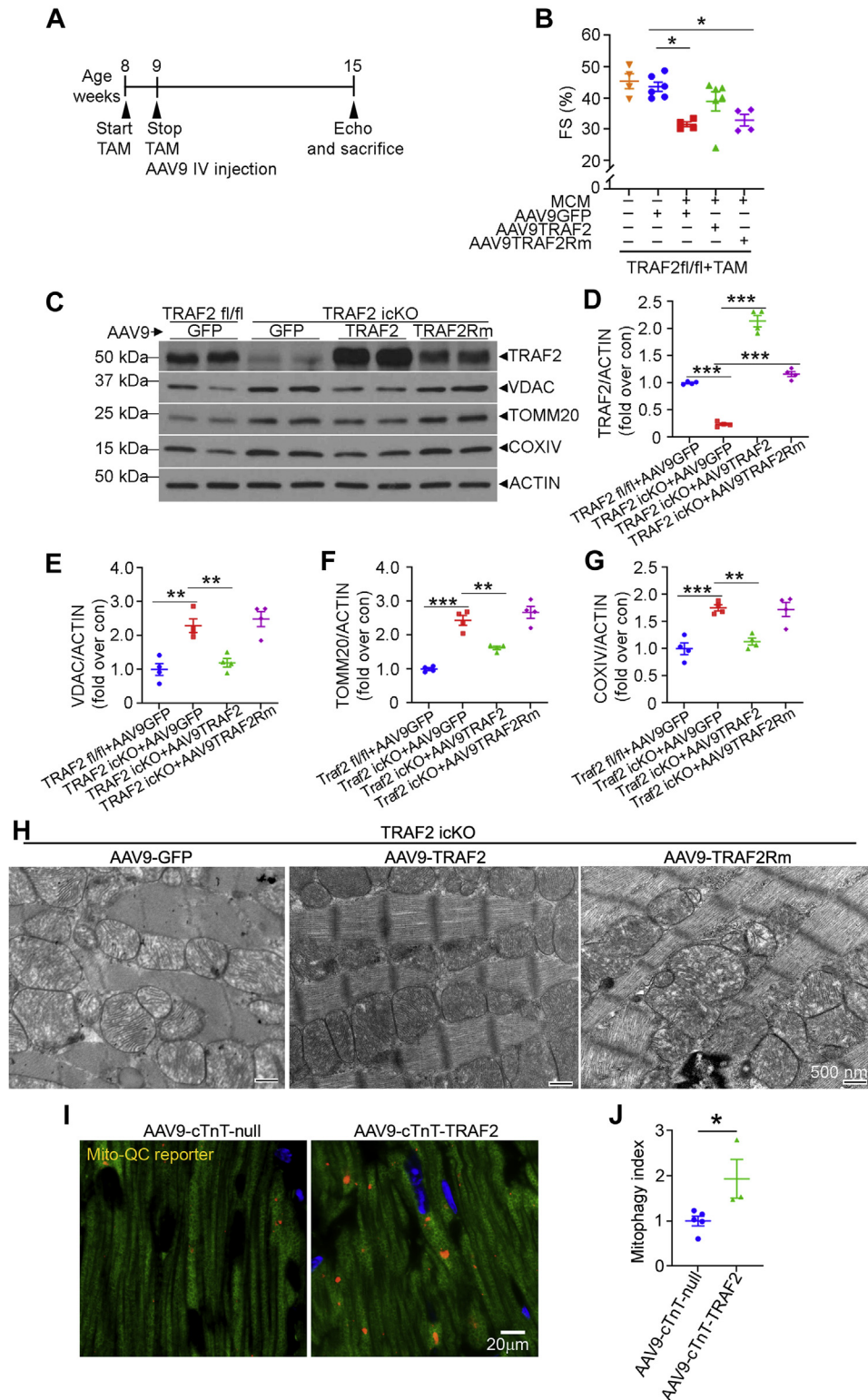
were then embedded in 10% gelatin and infiltrated overnight with 2.3 mol/L sucrose/20% polyvinyl pyrrolidone in PIPES/MgCl$_2$ at 4°C. Samples were trimmed, frozen in liquid nitrogen, and then sectioned with a Leica Ultracut UCT7 cryo-ultramicrotome (Leica Microsystems). Ultrathin sections of 50 nm were blocked with 5% FBS/5% NGS for 30 min and subsequently incubated with rabbit anti-GFP (Life Technologies, 1:200) for 1 hour at room temperature. Following washes in block buffer, sections were incubated with 18-nm colloidal gold conjugated goat anti-rabbit IgG+IgM (Jackson ImmunoResearch Laboratories, 1:30) for 1 hour. Sections were stained with 0.3% uranyl acetate/2% methyl cellulose and viewed on a JEOL 1200 EX transmission electron microscope (JEOL USA) equipped with an AMT 8 megapixel digital camera and AMT Image Capture Engine V602 software (Advanced Microscopy Techniques). All labeling experiments were conducted in parallel with control sections omitting the primary antibody.

STATISTICAL ANALYSIS. Data are presented as the mean ± SEM. All measurements were obtained on distinct biological replicates. Statistics were performed in Prism Version 8.0.2 (GraphPad Software). Data were tested for assumptions of normality with Shapiro-Wilk normality test. Statistical significance of differences was calculated via unpaired 2-tailed Student's *t*-test for 2 group comparisons, or 1-way or 2-way analysis of variance for assessing differences across multiple groups followed by post hoc testing (Tukey's) to evaluate pairwise differences. A nonparametric test was employed if data were not normally distributed. Graphs containing error bars show the mean ± SEM, with a *P* value <0.05 considered statistically significant. The datasets from the current study are available from the corresponding author on reasonable request.

RESULTS

Our published studies in isolated cardiomyocytes indicate that TRAF2, an innate immune adaptor, localizes to mitochondria.[26] To determine whether this occurs in human hearts, we obtained heart tissue from donors rejected for transplantation, as well as from patients with ischemic cardiomyopathy, and examined TRAF2 expression following biochemical fractionation into a mitochondria-enriched fraction, and cytosol (**Figures 1A to 1D**). TRAF2 protein was detected in the mitochondrial fraction, where it was dramatically up-regulated in hearts with ischemic cardiomyopathy and end-stage heart failure (**Figures 1B and 1D**). This was accompanied by an increase in overall TRAF2 levels (**Figures 1E and 1F**), as well as a relative decline in cytosolic levels (**Figures 1A and 1C**), suggesting that TRAF2 translocates to the mitochondria upon injury.

To examine the subcellular localization of TRAF2 in the mouse heart, we subjected wild-type mouse hearts to ex vivo ischemia-reperfusion injury or sham treatment and performed subcellular fractionation to further isolate the mitochondrial biochemical fraction into pure mitochondria, MAM and ER.[30] Our data (**Figures 1G and 1H**) demonstrate that TRAF2 is predominantly located in the pure mitochondrial fraction in the sham (unstressed) heart, with a lesser degree of localization to the MAM and ER. Ex vivo ischemia-reperfusion injury increased TRAF2 localization to mitochondria and the MAM (**Figures 1G and 1H**). Indeed, TRAF2 was also detected by immunogold analysis and transmission electron microscopy on mitochondrial membranes and MAM in HEK293 cells, with increased localization to these structures as well as to mitochondria in autophagosomes after hypoxia-reoxygenation injury (Supplemental Figure S1). These observations suggest that the stress-induced increase in TRAF2 localization to mitochondria may play a functional role in its cytoprotective effects, as suggested by prior studies showing that TRAF2 is both necessary[33] and sufficient[28,34,35] to enhance cardiomyocyte survival after ischemia-reperfusion injury.

To examine the mechanisms for recruitment of TRAF2 to the mitochondria, we evaluated whether its

---

FIGURE 7   Continued

(A) Schematic depicting experimental strategy for tamoxifen-inducible TRAF2 ablation in mice homozygous for floxed *Traf2* alleles carrying the *Myh6*-MerCreMer transgene, followed by AAV9-cTnT-TRAF2 or TRAF2Rm particles at 5.0 × 10^{11} viral particles per mouse. **(B)** Left ventricular endocardial fractional shortening (%FS) in TRAF2icKO mice or TRAF2 floxed mice transduced with AAV9 particles coding for TRAF2 or TRAF2Rm, driven by a cardiac troponin T promoter as shown in **A**. *$P < 0.05$ by post hoc test after 1-way ANOVA. **(C-G)** Representative immunoblot **(C)** with quantitation of TRAF2 expression **(D)** and abundance of mitochondrial proteins (VDAC, **E**; TOMM20, **F**; COXIV, **G**); all normalized to actin) in cardiac extracts from mice modeled as in **A**. **$P < 0.01$ and ***$P < 0.001$ by post hoc test after 1-way ANOVA. **(H)** Representative transmission electron microscopy images to evaluate myocardial ultrastructure in mice as in **A**. Scale bar = 500 nm. **(I and J)** Representative images **(I)** are shown demonstrating mitophagy with mitoQC reporter expression with quantitative assessment **(J)**, 4 weeks after injections of AAV9-cTnT-TRAF2 or empty viral particles (AAV9-cTnT-null) in 8-week-old mitoQC reporter mice. *$P < 0.05$ by *t*-test. Abbreviations as in **Figure 2**.

FIGURE 8   TRAF2 Ablation Induced Cell Death, Which Can Be Rescued by Parkin-Induced Mitophagy
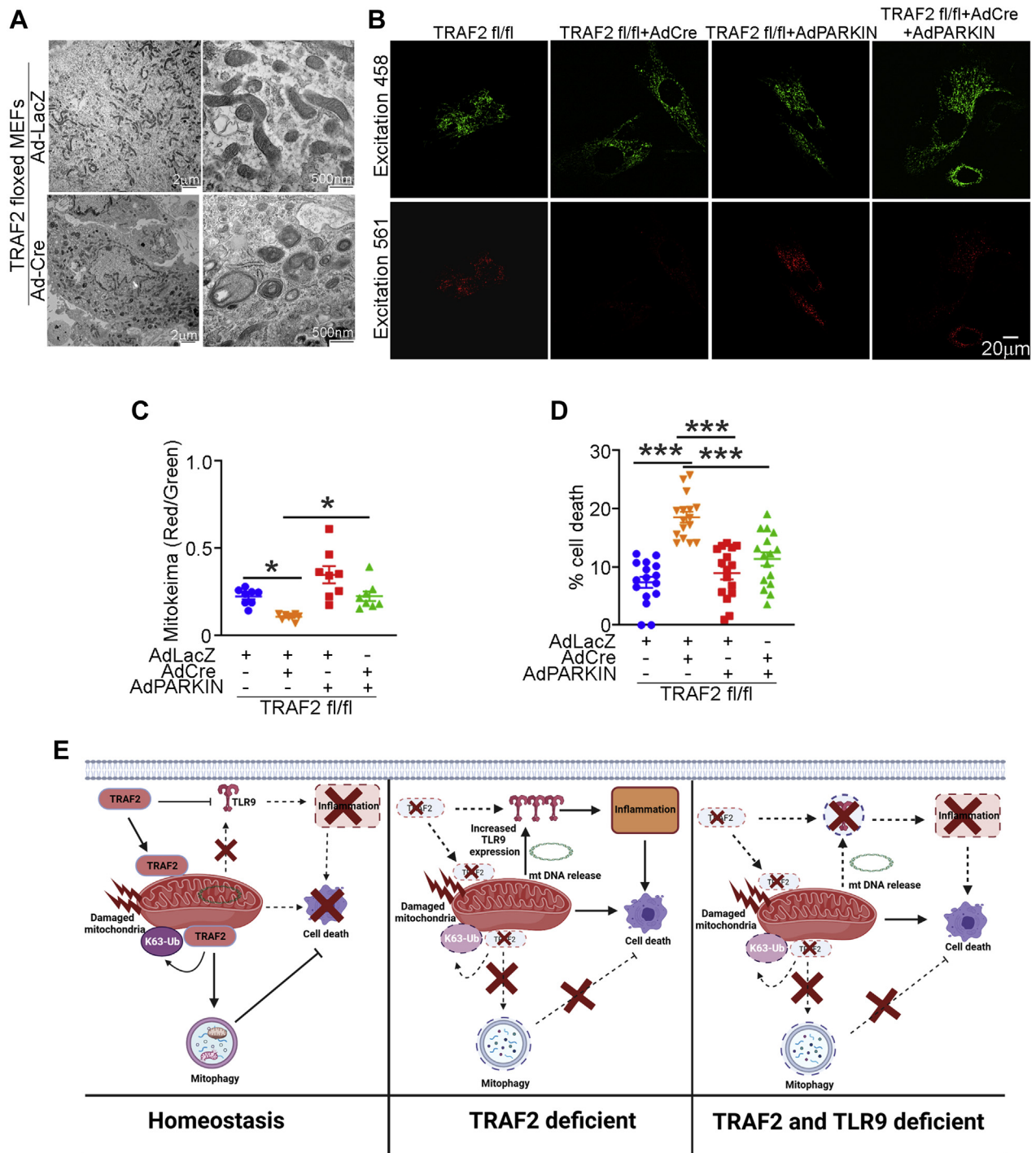
mitochondrial localization depends upon PINK1. Indeed, as an executor of the canonical mitophagy pathway via macro-autophagy, PINK1, a serine-threonine kinase, is stabilized upon inner membrane depolarization following mitochondrial damage and recruits the E3 ligase PARKIN.[36] PINK1 was not essential for recruitment of TRAF2 to the mitochondrial fraction under normoxic conditions, but loss of PINK1 markedly reduced TRAF2 translocation to the mitochondrial fraction upon hypoxia-reoxygenation injury (Supplemental Figure S2) consistent with a lack of role for PINK1 in executing basal mitophagy in the unstressed heart.[19] Taken together, these data suggest a role for TRAF2 in homeostatic mitochondrial quality control in cardiac myocytes, in vivo.

LOSS OF MYOCARDIAL TRAF2 IMPAIRS PHYSIOLOGICAL MITOPHAGY IN THE MOUSE HEART. Prior studies have determined that perinatal cardiomyocyte-specific ablation of TRAF2 in the mouse heart provokes necroptosis of cardiac myocytes with systemic inflammation and cardiomyopathy.[33] To isolate the effects of TRAF2 on cardiac myocyte homeostasis from developmental signaling, we examined the consequences of loss of TRAF2 in cardiomyocytes in the adult heart. Mice homozygous for floxed *Traf2* alleles carrying the *Myh6*-promoter-driven MCM were injected with tamoxifen (30 mg/kg/d) for 3 consecutive days to generate inducible cardiac-myocyte specific TRAF2 knockout mice (depicted as TRAF2-icKO). Similarly treated *Traf2* fl/fl mice (depicted as TRAF2 fl/fl) were studied as control mice. TRAF2-icKO mice manifest symptoms of heart failure with reduced physical activity, hunched posture, labored breathing, and ruffled coat within 5 days of initiating tamoxifen injections. Echocardiographic examination demonstrated marked LV cavity dilation and reduced contractile performance (% fractional shortening [% FS]) (Supplemental Figure S3A). On necropsy, the

hearts were enlarged with dilation of the LV cavity (Supplemental Figures S3B and S3C) and significantly increased heart weight (heart weight/tibial length ratio: 7.27 ± 0.5 in TRAF2-icKO mg/mm vs 5.66 ± 0.15 mg/mm in *Traf2* fl/fl, n = 3 per group; $P = 0.036$). Immunoblot analysis demonstrated a 66% reduction in myocardial TRAF2 protein in TRAF2-icKO mice (Supplemental Figures S4A and S4B). Although these data suggest that loss of TRAF2 results in cardiomyopathy, a decline in systolic performance was also detected in MCM transgenic mice as compared with wild-type alleles at the *Traf2* locus after tamoxifen injection (%FS: 30% ± 4% vs 51% ± 4% in wild-type control mice; $P = 0.016$ by *t*-test. n = 3/group).

Because this signal of Cre-mediated toxicity has been described previously,[37,38] we employed 2 other tamoxifen regimens that have been reported to circumvent Cre-mediated toxicity in the heart.[38,39] A 3-week regimen of IP tamoxifen injections (20 mg/kg/d for 5 days per week) resulted in a 70% reduction of in whole-heart TRAF2 levels (Supplemental Figures S4C and S4D). As expected, isolation of adult cardiomyocytes from nonmyocytes demonstrated near complete loss of TRAF2 protein in the cardiomyocyte fraction (Supplemental Figures S4E and S4F) in TRAF2-icKO mice. TRAF2 protein expression was not altered by MCM-mediated TRAF2 ablation in noncardiomyocytes (Supplemental Figures S4E and S4F). We observed increased mortality among TRAF2-icKO mice (5/13 vs 0/10 in *Traf2* fl/fl control mice; $P = 0.046$ by Fisher's exact test) with signs of heart failure such as reduced activity, labored breathing, and generalized swelling before death. None of the mice carrying the MCM transgene or *Traf2* fl/fl mice demonstrated signs of heart failure or died during the study. Serial echocardiography was performed at baseline, day 21 (after the last tamoxifen dose) and 2 weeks after the last dose was

FIGURE 8 Continued

(A) Murine embryonic fibroblasts (MEFs) carrying floxed *Traf2* alleles were modeled for TRAF2 ablation with adenoviral Cre (or LacZ as control, each at a multiplicity of infection [MOI] = 100) treatment for 72 hours as in Figure S11 and subjected to transmission electron microscopic (TEM) analysis. Representative TEM images are shown demonstrating mitochondrial abnormalities noted after *Traf2* ablation as compared with control mice. **(B and C)** Representative images **(B)** and quantitative analyses of mitoKeima emission in the red channel over green as an index of mitophagy **(C)**, in *Traf2*-null MEFs (modeled as in **A**) expressing mitoKeima transduced with adenoviral Parkin or LacZ (MOI = 100 for 48 hours) as control. Adenoviral particles coding for LacZ were added to equalize the number of viral particles per treatment. *$P < 0.05$ by post hoc test after 1-way ANOVA. **(D)** Cell death in *Traf2* null MEFs (modeled as in **A**) and transduced with adenoviral Parkin or LacZ (MOI = 100 for 72 hours) as control. Adenoviral particles coding for LacZ were added to equalize the number of viral particles per treatment. ***$P < 0.001$ by post hoc test after 1-way ANOVA. **(E)** Schematic depicting role of TRAF2-induced mitophagy in preventing inflammation and cell death in cardiac myocyte homeostasis. TRAF2 localizes to the mitochondria and promotes mitophagy via K63-ubiquitination activity in unstressed cardiac myocytes **(left)**. Ablation of TRAF2 results in mitochondrial DNA leak, and up-regulates TLR9 abundance to provoke inflammation via mitochondria DNA sensing. The resultant inflammation and accumulation of damaged mitochondria provoke cardiac myocyte cell death and cardiomyopathy **(middle)**. Concomitant ablation of TLR9 in the setting of TRAF2 deficiency prevents inflammation and cell death, and rescues left ventricular hypertrophy and function in the short term; but does not prevent accumulation of damaged mitochondria and cell death inexorably resulting in cardiomyopathy during follow up **(right)**.

administered. We observed a decline in LV contractile function as shown by %FS (**Figure 2A**) with LV dilation (**Figure 2B**) in TRAF2-icKO mice as compared with *Traf2* fl/fl control mice, that persisted at follow-up. We also observed a transient decline in %FS and mild LV dilation in transgenic MCM control mice, which was completely reversed at day 35 (**Figures 2A and 2B**), demonstrating evidence for transient, but reversible, Cre-mediated toxicity with this protocol. Surviving TRAF2-icKO mice demonstrated increased fibrosis at day 35 (**Figures 2C and 2D,** Supplemental Figure S5), and ultrastructural examination revealed abnormal swollen mitochondria with cristal rarefication (**Figure 2E**). This was accompanied by an ∼4-fold increase in TUNEL-positive cardiac myocytes as compared with *Traf2* fl/fl control mice (**Figure 2F**). Importantly, the myocardium in MCM transgenic mice was histologically indistinguishable from wild-type mice without an increase in TUNEL-positive cardiomyocytes (**Figures 2C to 2F**). Another regimen of a single dose of tamoxifen (40 mg/kg) followed by echocardiography 2 weeks later induced only a modest TRAF2 protein knockdown in the myocardium (Supplemental Figures S4G and S4H) and resulted in a mild cardiomyopathy with mildly dilated LV (3.6 ± 0.1 mm in TRAF2-icKO vs 3.3 ± 0.1 mm in *Traf2* fl/fl; $P = 0.017$, n = 4/group) with mild systolic dysfunction (%FS 41 ± 1 in TRAF2-icKO vs 50 ± 1 in *Traf2* fl/fl; $P < 0.001$). At this dose, we did not observe any cardiac structural or functional abnormalities in MCM transgenic mice as compared with wild-type control mice.

Overall, we observed a strong correlation between the degree of TRAF2 protein knockdown in the myocardium in the TRAF2-icKO mice and worsening fractional shortening and LV dilation (Supplemental Figures S4I and S4J) with different tamoxifen regimens. We also set up a model of inducible cardiac myocyte TRAF2 ablation by feeding tamoxifen chow. Mice treated with tamoxifen chow for 7 days demonstrated a similar degree of TRAF2 deletion as the 21-day injection regimen (Supplemental Figures S6A and S6B) and with comparable LV dilation and systolic dysfunction as compared with floxed control mice (data not shown). Taken together, these data indicate that the loss of TRAF2 in cardiac myocytes provokes cardiomyocyte death in unstressed hearts with spontaneous development of cardiomyopathy.

Prior studies with perinatal ablation of TRAF2 in cardiomyocytes (with *Myh6*-Cre) reported cardiac myocyte necrosis with systemic inflammation.[33] Accordingly, we assessed for circulating markers noted to be elevated with TRAF2 ablation in the prior work. Our data demonstrate that circulating HMGB1 levels, a marker of necrotic cell death (Supplemental Figure S7A), or circulating cytokines (IL-1β, TNF, and IL-6) (Supplemental Figures S7B to S7D) are not elevated in TRAF2-icKO mice as compared with *Traf2* fl/fl control mice, pointing to a different mechanism for the observed cardiomyopathy in mice with adult onset TRAF2 ablation.

We observed that mitochondrial proteins accumulate upon TRAF2 ablation in the TRAF2-icKO mice (**Figure 3A,** Supplemental Figures S6B to S6F), pointing to impaired removal of damaged mitochondria with TRAF2 deficiency (as seen with the TEM analysis in **Figure 2E**). Indeed, examination of basal mitophagy with AAV9-mediated transduction of mKeima reporter[32] revealed marked suppression of cardiac myocyte mitophagy in the TRAF2-icKO mice (**Figures 3B to 3D**). To determine whether the mitophagy deficit was secondary to defects in macro-autophagy, we examined flux in TRAF2-icKO mice expressing a dual fluorescent LC3-based flux reporter. The prevalence of autolysosomes relative to total autophagic structures, as well as the abundance of autolysosomes and autophagosomes, was not reduced in TRAF2-icKO as compared with *Traf2* fl/fl mice (**Figures 3E to 3G**). Moreover, the abundance of autophagosome-bound LC3-II and p62, an adaptor protein that binds to autophagic cargo to sequester them within autophagosomes, was not decreased (Supplemental Figures S8A to S8C); and transcripts for *Map1lc3b* (that encodes for LC3 protein), *Sqstm1* (which encodes for p62) and *Becn1* (which encodes for BECLIN-1, a protein essential for autophagosome formation) were not reduced in TRAF2-icKO hearts (Supplemental Figures S8D to S8F). These data indicate that the observed defect with TRAF2 ablation is with organelle-specific autophagy, that is, mitophagy, without impairment of macro-autophagy in TRAF2-icKO hearts.

TRAF2 ABLATION RESULTS IN MITOCHONDRIAL DNA RELEASE AND CARDIAC INFLAMMATION VIA TLR9. Impaired mitophagy results in mitochondrial DNA leak from damaged mitochondria, and TLR9-mediated mitochondrial DNA sensing has previously been shown to drive myocardial pathology under pressure overload stress.[2,4] TRAF2-icKO myocardium demonstrated increased co-localization of DNA detected by PicoGreen with TLR9 in cardiac myocytes (**Figure 4A**). Although PicoGreen is not specific for mitochondrial origin of the visualized DNA,[2] its cytosolic staining in the context of damaged mitochondria suggests release of mitochondrial DNA.

Furthermore, TRAF2 ablation resulted in transcriptional up-regulation of TLR9 expression (**Figures 4B to 4D**), which was localized to cardiac myocytes (**Figure 4E**) per in situ hybridization to detect *Tlr9* transcript expression.

To determine whether increased TLR9 activation led to increased inflammation, we assessed the prevalence of CD68+ macrophages. CD68+ cells were increased in TRAF2-icKO myocardium (**Figures 5A and 5B**), indicating increased inflammatory cell infiltrate. Concomitant ablation of TLR9 in TRAF2-icKO mice (Supplemental Figures S9A to S9C) markedly reduced cardiac CD68+ cells (**Figures 5A and 5B**) and TUNEL+ cardiomyocytes (**Figure 5C and 5D**) to levels observed in control mice. These data indicate that loss of TRAF2 sensitizes the myocardium to proinflammatory signaling driven by TLR9 sensing of leaked mitochondrial DNA.

Concomitant TLR9 ablation also attenuated the decline in systolic function (**Figure 5E**) and left ventricular hypertrophy (**Figures 5G and 5H**) without significantly affecting left ventricular dimensions (**Figure 5F**) in TRAF2-icKO mice. This was accompanied by reduced myocardial fibrosis (Supplemental Figures S9D-S9F). Assessment of the fetal gene expression program as a marker for pathologic hypertrophy showed reductions in *Nppa* (encoding for ANP), *Nppb* (encoding for BNP), *Acta1* (encoding for skeletal α-actin), and restoration of *Atp2a2* (encoding for SERCA2a) transcripts (**Figures 5I to 5L**), without an effect on *Myh6* and *Myh7* expression (Supplemental Figures S9G and S9H) in TRAF2-icKO mice with concomitant TLR9 expression versus those that were wild type at the *Tlr9* locus. Taken together, these data suggest that TLR9-mediated inflammatory cell infiltration in the myocardium drives cell death and myocardial pathology in TRAF2-icKO mice without a contribution from systemic inflammation driven by necroptotic cell death that was observed with perinatal TRAF2 ablation.[33]

Evaluation of mitochondrial ultrastructure revealed that concomitant ablation of TLR9 in TRAF2-icKO mice did not rescue the mitochondrial defects observed with TRAF2 ablation in cardiac myocytes (**Figures 2E and 6A**). Damaged mitochondria trigger cell death signaling,[1] which prompted us to follow these animals over a longer time period to determine whether impaired mitophagy would result in cardiomyopathy independent of TLR9-mediated inflammation. Re-examination of these animals at 36 weeks after tamoxifen treatment (to induce TRAF2 ablation) demonstrated LV dilation (**Figure 6B**), LV systolic dysfunction (**Figure 6C**), increased LV mass

(**Figure 6D**), and an increased ratio of cavity size to wall thickness (**Figure 6E**) in TRAF2-icKO-TLR9–null mice (as compared with control mice), indicating that persistence of damaged mitochondria is sufficient to induce cardiomyopathy independent of sustained inflammatory signaling.

AAV9-MEDIATED RESTORATION OF TRAF2, BUT NOT ITS E3 LIGASE–DEFICIENT MUTANT, RESCUES CARDIOMYOPATHY WITH CARDIOMYOCYTE TRAF2 ABLATION.

To gain a mechanistic understanding of whether TRAF2's E3 ligase function was critical, as we have observed previously in cardiomyocytes in cell culture,[26] we used an AAV9-based approach to restore TRAF2 expression in TRAF2-icKO myocardium. AAV9-mediated expression of TRAF2 targeted to cardiomyocytes with a cTnT promoter restored TRAF2 protein to levels ∼2-fold higher than in *Traf2* fl/fl mice treated with a control (AAV9-cTnT-GFP) viral particle (**Figures 7C and 7D**). AAV9-mediated expression of TRAF2 in TRAF2-icKO mice rescued the decline in systolic function (**Figures 7A and 7B**) and restored mitochondrial protein levels to those observed in control mice (**Figures 7C and 7E to 7G**). Mitochondrial morphology was also normalized in TRAF2-icKO mice with AAV9-mediated TRAF2 delivery (**Figure 7H**). In contrast, AAV9-mediated restoration of TRAF2 with ring domain mutations ablating its E3 ligase activity (ie, TRAF2-Rm mutant, as previously described[26,40]) (**Figure 7C**) did not rescue the systolic dysfunction (**Figures 7A and 7B**), restore abundance of mitochondrial proteins (**Figures 7C and 7E to 7G**), or rescue the mitochondrial defects (**Figure 7H**). These data demonstrate that the E3 ligase domain of TRAF2 is required for myocardial homeostasis and mitochondrial quality control, mirroring prior observations in isolated cultured primary cardiomyocyte.[26]

We next examined whether TRAF2 overexpression was sufficient to induce mitophagy in cardiac myocytes in the mouse heart. To test this, we employed AAV9-cTnT promoter-driven TRAF2 expression (**Figures 7C and 7D**) and compared that with expression of empty AAV9-cTnT null viral particles (as control) in hearts from mice expressing the mitoQC mitophagy reporter.[17] Our data demonstrate that exogenous TRAF2 is sufficient to induce mitophagy versus the control condition (**Figures 7I and 7J**).

PARKIN EXPRESSION IS NOT REDUNDANT TO TRAF2 FUNCTION; BUT EXOGENOUS PARKIN-INDUCED MITOPHAGY CAN RESCUE CELL DEATH WITH TRAF2 ABLATION.

In isolated cardiac myocytes, we have previously observed that TRAF2 colocalizes and

interacts with PARKIN in the setting of ionophore-induced mitochondrial damage.[26] We examined PARKIN levels in TRAF2-icKO mice and did not note them to be significantly altered (**Figure 3A**). To determine whether endogenous Parkin was playing role in the cardiomyopathy observed with TRAF2 ablation, we generated TRAF2-icKO mice in the *Park2* null (Parkin deficient) background. Loss of PARKIN did not worsen LV dysfunction or dilation, or affect histology or fibrosis in TRAF2-icKO mice (Supplemental Figure S10). These data are consistent with a lack of role for Parkin in basal mitophagy in cardiomyocytes in young adult mouse hearts.[8,21]

To determine whether the defective mitophagy induced by TRAF2 deficiency was responsible for increased cell death, we studied *Traf2* floxed MEFs (*Traf2* fl/fl MEFs), where TRAF2 was deleted with adenoviral-Cre expression (Supplemental Figure S11). Loss of TRAF2 in MEFs resulted in accumulation of damaged mitochondria by ultrastructural examination (**Figure 8A**) with impaired mitophagy assessed with mKeima expression (**Figures 8B and 8C**), and cell death (**Figure 8D**). Importantly, ablation of TRAF2 did not alter expression of LC3 or p62 two markers of macroautophagy (Supplemental Figure S11B) mirroring the findings in TRAF2-icKO mice (**Figures 3E to 3G**) and confirming a specific role for TRAF2 in mitophagy. Adenoviral overexpression of Parkin, as we have previously described,[26] rescued mitophagy to control levels and attenuated cell death with TRAF2 ablation (**Figures 8B to 8D**). Taken together, these data indicate that TRAF2 mediates mitophagy independent of Parkin, and the mitophagy defect is the proximate cause of cell death in the absence of TRAF2.

DISCUSSION

Purported as ancient symbionts, mitochondria act as arbiters of cellular viability and death.[1] In this work, we have identified a physiological role for mitophagy to remove damaged mitochondria in cardiomyocytes and distinguished the effects of inflammation from those due to persistent cell death signaling from damaged mitochondria in the development of cardiomyopathy. Our studies reveal a novel regulatory pathway that links 2 key elements of the innate immune system, namely TRAF2 and TLR9 to balance physiological mitophagy and suppress inflammatory signaling for maintaining myocardial homeostasis in the unstressed heart (**Figure 8E**).

These findings indicate that despite a vital role for mitochondria in energy generation in cardiac myocytes, rapid removal of damaged mitochondria via mitophagy is essential to maintain physiological functioning of the heart. TRAF2-mediated physiological mitophagy is also a critical mechanism to prevent sterile myocardial inflammation, provoked by sensing of mitochondrial DNA leaked from damaged mitochondria. This is particularly relevant because TLR9 signaling has been shown to drive inflammatory signaling in the setting of mitochondrial DNA release, when mitochondria are increasingly damaged, such as with pressure overload–induced stress or with ischemia-reperfusion injury.[2,4] Degradation of cytokine mRNAs by Regnase-1 is another mechanism to prevent sterile inflammation in the myocardium in the setting of pressure overload hypertrophy.[41] Curiously, although lysosomal DNase2a and Regnase-1 have been shown to be critical for protecting against myocardial inflammation under stress, mice deficient in these genes in cardiac myocytes do not have detectable myocardial inflammation, or cardiac structure or function abnormalities in the unstressed state.[2,41] These observations mimic the findings in the myocardium of unstressed adult *Pink1*- and *Park2*-null mice[7] and strongly support the contention that robust and efficient physiological mitophagy removes damaged mitochondria, to prevent mitochondrial DNA sensing and sterile inflammation, and maintain homeostasis. Our studies point to TRAF2 as the sensor that resides in the mitochondria to effect homeostatic mitophagy upon mitochondrial damage to prevent cardiac myocyte cell death. Indeed, TRAF2-mediated mitophagy prevents mitochondrial DNA release and DNA sensing to drive inflammation, as demonstrated with attenuation of myocardial CD68$^+$ macrophage abundance to levels seen in the unstressed state in TRAF2-icKO mice lacking TLR9. It is important to note that whereas TLR9 ablation rescued cardiac myocyte cell death in the short term by preventing mitochondrial DNA sensing and inflammation, the persistence of damaged mitochondria in the absence of TRAF2-induced mitophagy led to cardiomyopathy over a longer-term follow-up. These data underscore the critical importance for removal of damaged mitochondria to maintain cellular homeostasis.

TRAF2, an adaptor protein, has been ascribed critical roles in innate immunity and inflammatory signaling.[42] Our studies demonstrate a novel role for TRAF2 as the first mediator to be uncovered for transducing basal cardiac myocyte mitophagy in young adult mice, distinct from previously described roles for other pathways in stress-induced

mitophagy.[9-15] Similarly, TRAF2-mediated physiological mitophagy in young adult myocardium differs from mitophagy during perinatal cardiac growth and development[8] or mitophagy induced by exercise, a form of physiological stress.[7] Indeed, it is important to note the difference between basal and stress-induced mitophagy. In stress-induced mitophagy, prior studies describe a critical role for PINK1, a mitochondrially targeted serine-threonine kinase, which gets stabilized upon mitochondrial damage and recruits PARKIN,[43] an E3 ubiquitin ligase, that ubiquitinates mitochondrial proteins and targets the damaged mitochondria to autophagosomes.[44] Our data indicate that TRAF2 localizes to mitochondria independently of PINK1 in the unstressed state (Supplemental Figure S2) and mediates mitophagy independently of endogenous Parkin (Supplemental Figure S10). Moreover, exogenous TRAF2 is sufficient to induce mitophagy in cardiac myocytes (**Figures 7I and 7J**). Indeed, TRAF2 was uncovered in a screen for PINK1 and PARKIN-independent mitophagy mediators,[45] and inflammatory stimuli were observed to induce TRAF2-mediated mitophagy via ubiquitination of orphan nuclear receptor, Nur77,[46] independently confirming our prior observations that TRAF2 mediates mitophagy in cardiac myocytes in culture[26] and in unstressed hearts, in vivo (current dataset). Consistent with a role for PINK1-mediated mitophagy under stress, we found that PINK1 was essential for recruitment of TRAF2 to mitochondrial fraction upon hypoxia-reoxygenation injury, but did not affect TRAF2's localization to the mitochondria under unstressed normoxic conditions (Supplemental Figure S2).

Notably, our studies demonstrate induction of cellular inflammation with up-regulated macrophage abundance in the myocardium of mice with inducible adult-onset TRAF2 ablation, without evidence for systemic inflammation. These findings are in contrast to prior studies with perinatal ablation of TRAF2 in cardiac myocytes which demonstrate induction of systemic inflammation with increased circulating TNF levels (along with other cytokines) that transduces TNF receptor 1 (TNFR1)-mediated activation of cardiac myocyte necroptosis.[33] Similar observations were made in germline TRAF2-deficient mice[47] that demonstrate systemic inflammation, markedly elevated TNF-induced cell death, and early lethality. On the contrary, ablation of TRAF2 in myeloid cells,[48] hepatocytes,[49] or B cells[23] did not induce systemic inflammation, cell death, or mortality in unstressed mice. Taken together, these observations argue for developmental and/or cell-type specific effects of TRAF2 signaling in preventing necroptosis that are not observed in adult cardiac myocytes.

Our findings also confirm an important role for TRAF2's E3 ubiquitin ligase signaling function in facilitating mitophagy. TRAF2 facilitates K63 ubiquitination[50] and K63 poly-ubiquitination has been shown to selectively target proteins for lysosomal degradation.[51] We propose that the subcellular localization of TRAF2 mediates differential signaling through its E3 ligase activity. The fraction of TRAF2 that resides in the mitochondria acts as a sensor to effect physiological mitophagy upon mitochondrial damage to prevent mitochondrial DNA leak and cardiac myocyte cell death.

CONCLUSIONS

In summary, the data presented herein identify physiological cardiac myocyte mitophagy mediated by TRAF2 as an essential homeostatic phenomenon in the adult myocardium. In doing so, TRAF2 minimizes deleterious intracellular inflammatory signaling, both by preventing the accumulation of depolarized damaged mitochondria, as well as mitigating the impact of released mtDNA by suppressing the TLR9 levels to attenuate mtDNA sensing. A growing body of published reports supports a cardioprotective role for enhanced TRAF2 signaling in the setting of injury,[28,34,35] and TRAF2-stimulated mitophagy is likely to play an important role in transducing the observed benefits. Indeed, augmenting TRAF2 signaling to enhance mitochondrial quality control should be explored as a novel therapeutic strategy in cardiomyopathy.

administrative assistance with conducting the study. Graphical abstract was created with BioRender.com.

FUNDING SUPPORT AND AUTHOR DISCLOSURES

ADDRESS FOR CORRESPONDENCE: Dr Abhinav Diwan, Division of Cardiology, Washington University School of Medicine, 660 South Euclid Avenue, CSRB 827 NTA, St. Louis, Missouri 63110, USA. E-mail: adiwan@wustl.edu.

PERSPECTIVES

COMPETENCY IN MEDICAL KNOWLEDGE: Understanding the mediators of mitochondrial quality control in mitochondria-rich cardiac myocytes and their relevance to myocardial homeostasis is critical for targeting these pathways for clinical benefit. Our studies have uncovered the innate immune system, specifically the TRAF2 protein, as a first responder to mitochondrial damage and an effector of mitophagy, a lysosomal degradative process that removes damaged mitochondria. By facilitating mitophagy in cardiac myocytes, the innate immune response suppresses myocardial inflammation provoked by sensing of leaked mitochondrial DNA and prevents cardiac myocyte cell death triggered by activation of cell death signaling from persistence of damaged mitochondria.

TRANSLATIONAL OUTLOOK: We demonstrate that TRAF2-mediated mitophagy prevents myocardial inflammatory cell infiltration and cardiac myocyte death, which are recognized pathophysiological mechanisms for development of cardiomyopathy and its progression to heart failure. Taken together with prior preclinical reports demonstrating cardioprotective effects of modest activation of TRAF2 signaling under stress, these studies support a translational strategy for enhancing TRAF2-mediated mitophagy to suppress inflammation and prevent cell death to treat heart failure.

REFERENCES

1. Del Re DP, Amgalan D, Linkermann A, Liu Q, Kitsis RN. Fundamental mechanisms of regulated cell death and implications for heart disease. *Physiol Rev*. 2019;99:1765–1817.

2. Oka T, Hikoso S, Yamaguchi O, et al. Mitochondrial DNA that escapes from autophagy causes inflammation and heart failure. *Nature*. 2012;485:251–255.

3. Diwan A, Wansapura J, Syed FM, Matkovich SJ, Lorenz JN, Dorn GW. Nix-mediated apoptosis links myocardial fibrosis, cardiac remodeling, and hypertrophy decompensation. *Circulation*. 2008;117: 396–404.

4. Kitazume-Taneike R, Taneike M, Omiya S, et al. Ablation of Toll-like receptor 9 attenuates myocardial ischemia/reperfusion injury in mice. *Biochem Biophys Res Comm*. 2019;515:442–447.

5. Diwan A, Krenz M, Syed FM, et al. Inhibition of ischemic cardiomyocyte apoptosis through targeted ablation of Bnip3 restrains postinfarction remodeling in mice. *J Clin Invest*. 2007;117:2825–2833.

6. Adamo L, Rocha-Resende C, Prabhu SD, Mann DL. Reappraising the role of inflammation in heart failure. *Nat Rev Cardiol*. 2020;17:269–285.

7. Sliter DA, Martinez J, Hao L, et al. Parkin and PINK1 mitigate STING-induced inflammation. *Nature*. 2018;561:258–262.

8. Gong G, Song M, Csordas G, Kelly DP, Matkovich SJ, Dorn GW 2nd. Parkin-mediated mitophagy directs perinatal cardiac metabolic maturation in mice. *Science*. 2015;350:aad2459.

9. Hoshino A, Wang WJ, Wada S, et al. The ADP/ATP translocase drives mitophagy independent of nucleotide exchange. *Nature*. 2019;575:375–379.

10. Kubli DA, Quinsay MN, Gustafsson AB. Parkin deficiency results in accumulation of abnormal mitochondria in aging myocytes. *Commun Integr Biol*. 2013;6:e24511.

11. Hoshino A, Mita Y, Okawa Y, et al. Cytosolic p53 inhibits Parkin-mediated mitophagy and promotes mitochondrial dysfunction in the mouse heart. *Nat Commun*. 2013;4:2308.

12. Kubli DA, Zhang X, Lee Y, et al. Parkin protein deficiency exacerbates cardiac injury and reduces survival following myocardial infarction. *J Biol Chem*. 2013;288:915–926.

13. Tong M, Saito T, Zhai P, et al. Mitophagy is essential for maintaining cardiac function during high fat diet-induced diabetic cardiomyopathy. *Circ Res*. 2019;124:1360–1371.

14. Shirakabe A, Zhai P, Ikeda Y, et al. Drp1-dependent mitochondrial autophagy plays a protective role against pressure overload-induced mitochondrial dysfunction and heart failure. *Circulation*. 2016;133:1249–1263.

15. Song M, Gong G, Burelle Y, et al. Interdependence of parkin-mediated mitophagy and mitochondrial fission in adult mouse hearts. *Circ Res*. 2015;117(4):346–351.

16. Sun N, Yun J, Liu J, et al. Measuring in vivo mitophagy. *Mol Cell*. 2015;60:685–696.

17. McWilliams TG, Prescott AR, Allen GFG, et al. mito-QC illuminates mitophagy and mitochondrial

architecture in vivo. *J Cell Biol*. 2016;214:333–345.

18. Narendra D, Tanaka A, Suen DF, Youle RJ. Parkin is recruited selectively to impaired mitochondria and promotes their autophagy. *J Cell Biol*. 2008;183(5):795–803.

19. McWilliams TG, Prescott AR, Montava-Garriga L, et al. Basal mitophagy occurs independently of PINK1 in mouse tissues of high metabolic demand. *Cell Metab*. 2018;27:439–449.e5.

20. Woodall BP, Orogo AM, Najor RH, et al. Parkin does not prevent accelerated cardiac aging in mitochondrial DNA mutator mice. *JCI Insight*. 2019;5(10):e127713.

21. Kubli DA, Cortez MQ, Moyzis AG, Najor RH, Lee Y, Gustafsson AB. PINK1 is dispensable for mitochondrial recruitment of parkin and activation of mitophagy in cardiac myocytes. *PLoS One*. 2015;10:e0130707.

22. Ng MYW, Wai T, Simonsen A. Quality control of the mitochondrion. *Dev Cell*. 2021;56:881–905.

23. Grech AP, Amesbury M, Chan T, Gardam S, Basten A, Brink R. TRAF2 differentially regulates the canonical and noncanonical pathways of NF-kappaB activation in mature B cells. *Immunity*. 2004;21:629–642.

24. Sohal DS, Nghiem M, Crackower MA, et al. Temporally regulated and tissue-specific gene manipulations in the adult and embryonic heart using a tamoxifen-inducible Cre protein. *Circ Res*. 2001;89:20–25.

25. Ma X, Mani K, Liu H, et al. Transcription factor EB activation rescues advanced alphaB-crystallin mutation-induced cardiomyopathy by normalizing desmin localization. *J Am Heart Assoc*. 2019;8:e010866.

26. Yang KC, Ma X, Liu H, et al. Tumor necrosis factor receptor-associated factor 2 mediates mitochondrial autophagy. *Circ Heart Fail*. 2015;8:175–187.

27. Prasad KM, Xu Y, Yang Z, Acton ST, French BA. Robust cardiomyocyte-specific gene expression following systemic injection of AAV: in vivo gene delivery follows a Poisson distribution. *Gene Ther*. 2011;18(1):43–52.

28. Evans S, Tzeng HP, Veis DJ, et al. TNF receptor-activated factor 2 mediates cardiac protection through noncanonical NF-κB signaling. *JCI Insight*. 2018;3(3):e98278.

29. Brunet S, Aimond F, Li H, et al. Heterogeneous expression of repolarizing, voltage-gated K+ currents in adult mouse ventricles. *J Physiol*. 2004;559:103–120.

30. Wieckowski MR, Giorgi C, Lebiedzinska M, Duszynski J, Pinton P. Isolation of mitochondria-associated membranes and mitochondria from animal tissues and cells. *Nature Protoc*. 2009;4:1582–1590.

31. Javaheri A, Bajpai G, Picataggi A, et al. TFEB activation in macrophages attenuates post-myocardial infarction ventricular dysfunction independently of ATG5-mediated autophagy. *JCI Insight*. 2019;4(21):e127312.

32. Shirakabe A, Fritzky L, Saito T, et al. Evaluating mitochondrial autophagy in the mouse heart. *J Mol Cell Cardiol*. 2016;92:134–139.

33. Guo X, Yin H, Li L, et al. Cardioprotective role of tumor necrosis factor receptor-associated factor 2 by suppressing apoptosis and necroptosis. *Circulation*. 2017;136:729–742.

34. Burchfield JS, Dong JW, Sakata Y, et al. The cytoprotective effects of tumor necrosis factor are conveyed through tumor necrosis factor receptor-associated factor 2 in the heart. *Circ Heart Fail*. 2010;3:157–164.

35. Tzeng HP, Evans S, Gao F, et al. Dysferlin mediates the cytoprotective effects of TRAF2 following myocardial ischemia reperfusion injury. *J Am Heart Assoc*. 2014;3:e000662.

36. Lazarou M, Sliter DA, Kane LA, et al. The ubiquitin kinase PINK1 recruits autophagy receptors to induce mitophagy. *Nature*. 2015;524:309–314.

37. Koitabashi N, Bedja D, Zaiman AL, et al. Avoidance of transient cardiomyopathy in cardiomyocyte-targeted tamoxifen-induced MerCreMer gene deletion models. *Circ Res*. 2009;105:12–15.

38. Lexow J, Poggioli T, Sarathchandra P, Santini MP, Rosenthal N. Cardiac fibrosis in mice expressing an inducible myocardial-specific Cre driver. *Dis Mod Mech*. 2013;6(6):1470–1476.

39. Schugar RC, Moll AR, Andre d'Avignon D, Weinheimer CJ, Kovacs A, Crawford PA. Cardiomyocyte-specific deficiency of ketone body metabolism promotes accelerated pathological remodeling. *Mol Metab*. 2014;3:754–769.

40. Habelhah H, Takahashi S, Cho SG, Kadoya T, Watanabe T, Ronai Z. Ubiquitination and translocation of TRAF2 is required for activation of JNK but not of p38 or NF-kappaB. *EMBO J*. 2004;23:322–332.

41. Omiya S, Omori Y, Taneike M, et al. Cytokine mRNA degradation in cardiomyocytes restrains sterile inflammation in pressure-overloaded hearts. *Circulation*. 2020;141:667–677.

42. Yang XD, Sun SC. Targeting signaling factors for degradation, an emerging mechanism for TRAF functions. *Immunol Rev*. 2015;266:56–71.

43. Narendra DP, Jin SM, Tanaka A, et al. PINK1 is selectively stabilized on impaired mitochondria to activate Parkin. *PLoS Biol*. 2010;8:e1000298.

44. Moyzis AG, Sadoshima J, Gustafsson AB. Mending a broken heart: the role of mitophagy in cardioprotection. *Am J Physiol Heart Circ Physiol*. 2015;308(3):H183–H192.

45. Zachari M, Gudmundsson SR, Li Z, et al. Selective autophagy of mitochondria on a ubiquitin-endoplasmic-reticulum platform. *Dev Cell*. 2020;55:251.

46. Hu M, Luo Q, Alitongbieke G, et al. Celastrol-induced Nur77 interaction with TRAF2 alleviates inflammation by promoting mitochondrial ubiquitination and autophagy. *Mol Cell*. 2017;66:141–153.e6.

47. Yeh WC, Shahinian A, Speiser D, et al. Early lethality, functional NF-kappaB activation, and increased sensitivity to TNF-induced cell death in TRAF2-deficient mice. *Immunity*. 1997;7:715–725.

48. Jin J, Xiao Y, Hu H, et al. Proinflammatory TLR signalling is regulated by a TRAF2-dependent proteolysis mechanism in macrophages. *Nat Commun*. 2015;6:5930.

49. Chen Z, Sheng L, Shen H, et al. Hepatic TRAF2 regulates glucose metabolism through enhancing glucagon responses. *Diabetes*. 2012;61:566–573.

50. Alvarez SE, Harikumar KB, Hait NC, et al. Sphingosine-1-phosphate is a missing cofactor for the E3 ubiquitin ligase TRAF2. *Nature*. 2010;465:1084–1088.

51. Nathan JA, Kim HT, Ting L, Gygi SP, Goldberg AL. Why do cellular proteins linked to K63-polyubiquitin chains not associate with proteasomes? *EMBO J*. 2013;32:552–565.

KEY WORDS cell death, inflammation, mitophagy, TRAF2

APPENDIX For supplemental tables and figures, please see the online version of this paper.